

NASA/TM—1998-207924



# Thickness-Independent Ultrasonic Imaging Applied to Abrasive Cut-Off Wheels: An Advanced Aerospace Materials Characterization Method for the Abrasives Industry

A NASA Lewis Research Center  
Technology Transfer Case History

Don J. Roth  
Lewis Research Center, Cleveland, Ohio

Donald A. Farmer  
Allison Abrasives, Inc., Lancaster, Kentucky

National Aeronautics and  
Space Administration

Lewis Research Center

---

August 1998

Trade names or manufacturers' names are used in this report for identification only. This usage does not constitute an official endorsement, either expressed or implied, by the National Aeronautics and Space Administration.

Available from

NASA Center for Aerospace Information  
7121 Standard Drive  
Hanover, MD 21076  
Price Code: A03

National Technical Information Service  
5287 Port Royal Road  
Springfield, VA 22100  
Price Code: A03

THICKNESS-INDEPENDENT ULTRASONIC IMAGING APPLIED TO ABRASIVE CUT-OFF WHEELS:  
AN ADVANCED AEROSPACE MATERIALS CHARACTERIZATION METHOD FOR  
THE ABRASIVES INDUSTRY

A NASA LEWIS RESEARCH CENTER TECHNOLOGY TRANSFER CASE HISTORY

Don J. Roth  
NASA Lewis Research Center  
MS 6-1  
21000 Brookpark Rd.  
Cleveland, OH 44135  
ph: 216-433-6017  
email: don.j.roth@lerc.nasa.gov  
and  
Donald A. Farmer, Chairman  
Allison Abrasives, Inc.  
163 Industry Rd.  
Lancaster, KY 40444  
ph: 606-792-3033

ABSTRACT

Abrasive cut-off wheels are at times unintentionally manufactured with nonuniformity that is difficult to identify and sufficiently characterize without time-consuming, destructive examination. One particular nonuniformity is a density variation condition occurring around the wheel circumference or along the radius, or both. This density variation, depending on its severity, can cause wheel warpage and wheel vibration resulting in unacceptable performance and perhaps premature failure of the wheel. Conventional nondestructive evaluation methods such as ultrasonic c-scan imaging and film radiography are inaccurate in their attempts at characterizing the density variation because a superimposing thickness variation exists as well in the wheel. In this article, the single transducer thickness-independent ultrasonic imaging method, developed specifically to allow more accurate characterization of aerospace components, is shown to precisely characterize the extent of the density variation in a cut-off wheel having a superimposing thickness variation. The method thereby has potential as an effective quality control tool in the abrasives industry for the wheel manufacturer.

INTRODUCTION AND BACKGROUND

A Problem for the Abrasives Industry in the Manufacture of Abrasive Cut-off Wheels

Abrasive cut-off wheels are used extensively to cut materials of all types. The cutting requires that the wheel rotate at relatively high speeds (usually in the range 6000 to 16000 surface feet per minute). It is therefore important that the wheel is flat (not warped) and in balance so as not to wobble and vibrate in use. Wobble and vibration at these speeds can result in crooked cuts, and in extreme cases, cause the wheel to break. Warpage and/or an out-of-balance condition are caused principally by variations in density (porosity) across the wheel. High densities near the bore (center) will usually result in wheel warpage; areas of non-uniform density around the circumference can result in an out-of-balance condition. Density variation across a wheel is difficult to characterize without destructive and time-consuming sectioning to perform either immersion density measurements or optical examination of pore fraction. A nondestructive evaluation (NDE) method would be desirable to gauge the extent of nonuniformity throughout the entire wheel and allow conclusions to be drawn regarding wheel usability.

The Difficulty With Conventional NDE methods

Conventional NDE methods such as ultrasonic c-scan imaging and film radiography are ineffective in characterizing the degree of density variation in such cut-off wheels because the wheels contain a superimposing thickness variation which the conventional NDE methods cannot separate from microstructural variation.

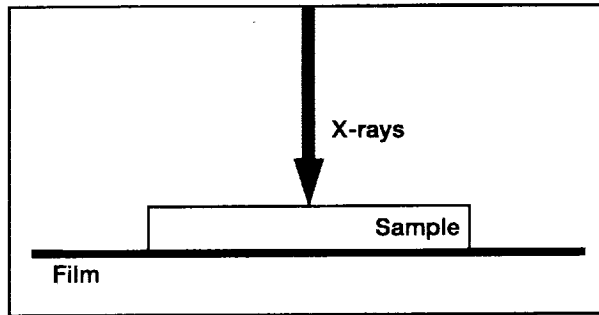


Figure 1.—Conventional film radiographic set-up.

For conventional film radiography where a source of photons impinges on a material sample from one side and x-ray film is present on the opposite sample surface (Figure 1), the governing equation shows the exponential dependence of transmitted x-rays on material density ( $\rho$ ) and thickness according to (Macovski, 1983):

$$N = N_0 \exp[-(K)(\rho d)] \quad (1)$$

where  $N$  is the number of photons arriving at the film;  $N_0$  is the total number of impinging photons;  $K$  is a constant determined by Avogadro's number, the total cross section atomic attenuation coefficient (proportionality constant), and the atomic weight of the material;  $\rho$  is the material density, and  $d$  is material thickness. Interpretation of the conventional radiograph is difficult as thickness variation effects can mask or overemphasize the true microstructural variation portrayed in the radiographic image of a part containing thickness variation. For example, increasing thickness and increasing density are complementary effects regarding the number of photons arriving at the film, i.e. both effects would cause a decrease in the number of arriving photons.

For conventional pulse-echo ultrasonic time-of-flight imaging where front and back surface echoes are gated (Figure 2), the linear effect of thickness is easily observed from the equation for pulse-echo waveform time-of-flight ( $2t$ ) (between the first front surface echo (FS) and the first back surface echo (B1), or between two successive back surface echoes (B1, B2)):

$$2\tau = \frac{2d}{V} \quad (2)$$

where  $d$  is the material thickness and  $V$  is the velocity of ultrasound in the material. In Equation (2),  $2\tau$  is directly proportional to thickness.  $2\tau$  will also be affected by microstructural factors such as density variation since ultrasonic velocity ( $V$ ) has been shown to be directly proportional to material density for a given material (Roth, et al., 1991).

Thickness effects on time-of-flight can also be interpreted by rearranging Equation (2) to calculate *apparent* velocity according to:

$$V = \frac{2d}{2\tau} \quad (3)$$

For velocity mapping from scan results, only one thickness value can be used practically in the velocity map calculation (Equation (2)). This value is usually an average value obtained from several measurements at different sample locations. For scan locations where actual thickness is less than the value chosen for the calculation,  $2\tau$  will be less and *apparent* velocity will be greater, than those if the scan location had the chosen value of thickness. The situation is opposite for scan locations where actual thickness is greater than the value chosen for the calculation. Thus, as for the conventional radiograph, interpretation of the time-of-flight or *apparent* velocity image is difficult as thickness variation effects can mask or overemphasize the true microstructural variation portrayed in the image of a part containing thickness variation. For example, increasing thickness and increasing density are effects that compete directly against each other for velocity.

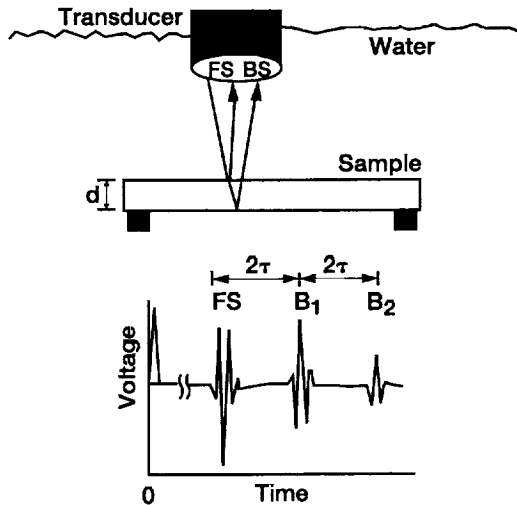


Figure 2.—Conventional pulse-echo ultrasonic measurement set-up.

Ultrasonic peak amplitude is dependent on sample thickness according to the exponential expression for ultrasonic attenuation (for the pulse-echo set-up shown in Figure 2) (Green and McIntire, 1991):

$$A = A_0 \exp(-\alpha[2d]) \quad (4)$$

where  $A$  is the received peak amplitude after traveling through to the sample back surface and back to the transducer,  $A_0$  is the initial reference amplitude,  $\alpha$  is the material attenuation coefficient that will vary as a function of microstructural condition, and  $d$  is material thickness. In practical application, the severity of the effect of thickness variation on peak amplitude depends on the frequency of ultrasound used because the ultrasonic attenuation coefficient ( $\alpha$ ) normally increases with increasing frequency (Roth, 1996). The lower the transducer frequency employed, the less significant thickness variation effects will be. Also, however, as the transducer frequency is decreased, sensitivity towards and resolution of nonuniformity generally decreases.

Note that an advanced NDE method, x-ray computed tomography (Macovski, 1983), can discern between thickness and density variation in components. However, tomography can be extremely time-consuming and expensive to apply, and is prone to artifacts under some conditions.

#### The Single-Transducer Thickness-Independent Ultrasonic Imaging Method

The single-transducer thickness-independent ultrasonic imaging method has been developed to an advanced degree at NASA Lewis Research Center and commercialized via a formal collaborative agreement between NASA and Sonix, Inc. (Roth, 1996). Its applications to structures of plate- and curved/tubular-geometry at NASA have been described in detail (Roth, 1996; 1997; 1998). To provide the reader some brief background on the method, several studies (Sollish, 1977; Pichè, 1984; Kuo, Hete, Shung, 1992; Hsu and Hughes, 1992) described a single point ultrasonic velocity measurement method using a reflector plate located behind and separated from the sample, that does not require prior knowledge of sample thickness. The latter method was studied with success in prototypical scanning configurations for plate-like shapes (Dayal, 1992; Hughes, and Hus, 1994; Roth, 1997), and incorporated into a commercial scan system (Roth, 1996). Figure 3 shows a schematic of the immersion pulse-echo testing set-up required to use this method and the resulting ultrasonic waveforms. The mathematical derivation for the method (Roth, 1997) results in ultrasonic velocity being calculated according to:

$$V = c \left( \frac{\Delta t}{2\tau} + 1 \right) \quad (5)$$

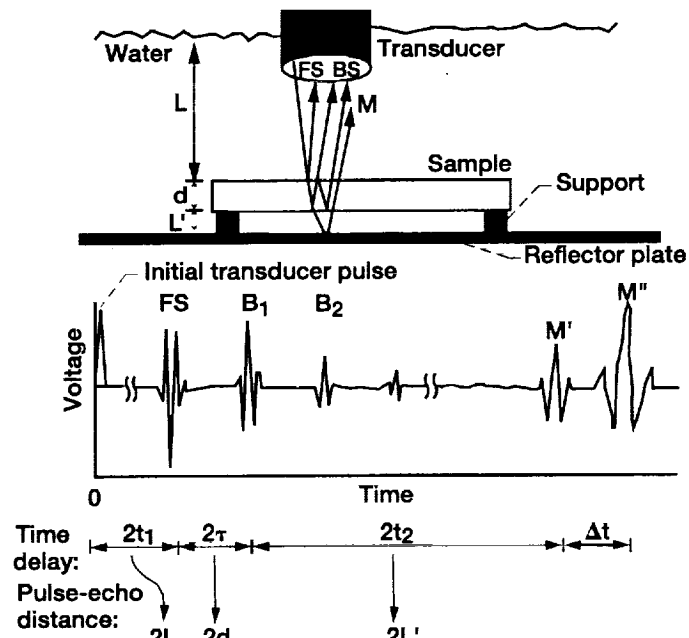


Figure 3.—Single-transducer thickness-independent ultrasonic measurement set-up.

where  $c$  is water velocity,  $2\tau$  is the pulse-echo waveform time-of-flight between the first front surface echo (FS) and the first back surface echo (B1), or between two successive back surface echoes (B1, B2), and  $\Delta t$  is the pulse-echo time-of-flight difference between the first echo off the reflector plate front surface with ( $M'$ ) and without ( $M''$ ) the sample present, respectively. Water velocity ( $c$ ) is determined from known relations between water velocity and temperature (Green and McIntire, 1991) or by direct measurement using the time difference of ultrasonic wave travel between two transducer linear positions. This thickness-independent ultrasonic imaging method does not require prior knowledge of sample thickness as shown in Equation (4), and if engineered for scanning, the effect of thickness variation is eliminated in the resulting image. Precision and relative accuracy associated with this method are estimated at near 1 percent for plate-like samples with machined surfaces (Roth, 1997).

#### How Allison Abrasives, Inc. Found out About The Single-Transducer Thickness-independent Method

Technology transfer "where it makes sense" is a significant current priority of NASA as stated by the Director of NASA in the NASA strategic plan (NASA Strategic Plan, 1995). One means by which NASA publicly advertises its technological advancements is via the monthly NASA Tech Briefs magazine. In one such issue (NASA Tech Brief, 1997), NASA had published a summary describing the single transducer thickness-independent ultrasonic imaging method. The tech brief article was noticed by representatives of the abrasives industry who contacted NASA regarding the use of this method to nondestructively characterize microstructural variation in abrasive cut-off wheels.

### EXPERIMENTAL

#### Materials

An optical photograph of an abrasive cut-off wheel is shown in Figure 4. The wheel is composed of aluminum oxide particles embedded into a polymeric substance. Surface roughness variations are present in the wheel as the central region appears smoother in some areas than in the surrounding region. A thickness profile along a line (shown) nearly through the center of the wheel from left edge to right edge is shown in Figure 5. It is seen that the cut-off wheel is thicker at the center than at the areas surrounding the center by about 0.2 mm (10%).

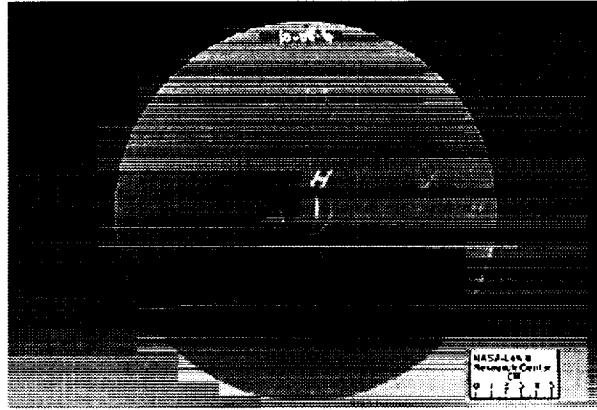


Figure 4.—Optical photograph of abrasive cut-off wheel. (Line shown is that where thickness profile was measured as shown in figure 5.)

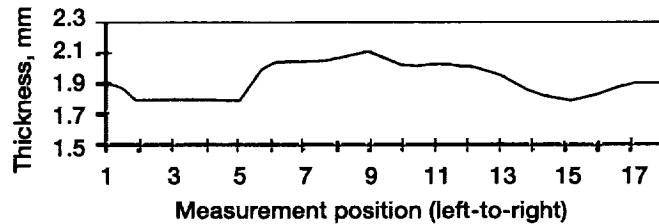


Figure 5.—Thickness vs. position number along the line shown in figure 4 (edge to edge) for the grinding wheel.

### Ultrasonic Imaging

The wheel underwent conventional pulse-echo ultrasonic peak amplitude and time-of-flight (TOF) c-scanning, followed by the single transducer thickness-independent ultrasonic imaging. The TOF c-scan was used to form an apparent velocity image by inputting an average thickness ( $d$ ) for the wheel during the velocity image calculation (Equation (3)). The scanning was done using a Sonix, Inc. ultrasonic scan system with a Sonix, Inc. 81g 1 GHz analog-to-digital converter board. Scans were performed in the orientation shown in the photograph of Figure 4 with the side showing the sample ID facing the transducer and the ID located at the top of the wheel. The following general scan parameters were used: 2.25 MHz broadband transducer ( $\sim 1$  to 2 mm ultrasonic wavelength ( $\lambda$ ) in the abrasive cut-off wheel [from  $\lambda = V/f$  where  $V$  is the  $\sim$  ultrasonic velocity in this type of wheel and  $f$  is the nominal transducer center frequency]); 250 MHz analog-to-digital sampling rate (4  $\eta$ sec time resolution); first front surface echo (FS), first back surface echo (B1), and reflector echoes  $M'$  and  $M''$  gated to acquire peak amplitude and/or TOF associated with these echoes; 0.25 mm scan increment (c-scan) and 1 mm scan increment (thickness-independent). For thickness-independent ultrasonic imaging, a circular stainless steel plate of larger diameter than the cut-off wheel was used as the reflector plate. Three scans were used to obtain all echo time-of-flight information as required using the version of this method that is commercially-available (Roth, 1996). The  $2\tau$  TOF difference (DTOF) (Equation (2)) between echoes FS and B1 was obtained using negative cross-correlation in scan 1 (because FS and B1 were phase inverted).  $M'$  and  $M''$  time-of-flights (TOF) were obtained using TOF to the positive peak in scans 2 and 3, respectively. Subtracting  $M'$  TOF from  $M''$  TOF at corresponding positions gave  $\Delta t$  (Equation (5)).

## Film radiography

Conventional film radiography through the thickness of the abrasive cut-off wheel was performed over the wheel (orientation as shown in photograph of Figure 4) with the film placed against the back side of the wheel. Parameters for the film radiography were tube voltage = 28 kV, current = 7 ma, 0.7 mm focal spot, exposure time = 2 min, source-to-film distance = 122 cm, and use of M film. The radiographic image was digitized using an x-ray digitizing system and x-ray transmission density (XD) line profiles obtained from (Halmshaw, 1982):

$$XD = G_D \log \frac{I_0}{I_t} \quad (6)$$

where  $I_0$  is the incident light intensity on the x-ray film negative,  $I_t$  is the transmitted light through the film and  $G_D$  is the slope of the film characteristic curve (film gradient).

## RESULTS AND DISCUSSION

Figure 6 compares for the cut-off wheel a conventional pulse-echo ultrasonic c-scan peak amplitude image (B1 gated), an apparent velocity image, a film radiograph, and a thickness-independent ultrasonic velocity image. All figures also show line profiles of the NDE property at a horizontal position near the center of the corresponding image of the wheel.

Upon initial examination, the peak amplitude c-scan image (Figure 6a, shown with 235 shades of gray) and peak amplitude line profile do not clearly indicate any major difference between the central and surrounding regions in the wheel. However, significant peak amplitude variations are present (note dark and light regions). The apparent velocity image (Figure 6b, shown with the gray scale manipulated in ~ thresholding-type fashion to highlight the nonuniformity shown in the image) and velocity line profile indicate a central region of lower velocity as compared to the surrounding region. This result correlates with the greater thickness measured in the central region (Figure 5) and thus is consistent with Equations (2) and (3) where greater thickness leads to greater  $2\tau$ . The film radiographic image (Figure 6c, shown with 255 shades of gray) and x-ray density line profile (Equation (5)) of the cut-off wheel indicate the central region to have lower x-ray density (average of ~1.8) than the surrounding region (average of ~2.2). This result, like that for apparent velocity, correlates with greater thickness (Figure 5) in the wheel center and thus is consistent with Equation (3). The thickness-independent velocity image (Figure 6d, shown with 235 shades of gray) and velocity line profile show higher velocity in a significant portion of the central region compared to the surrounding region. This result is the opposite of that seen in the apparent velocity image (Figure 6b) where relatively low velocity is shown in the central region due to the greater thickness in the central region. From these results, an initial conclusion can be drawn: the true microstructural variation in the apparent velocity image of the wheel is masked by the superimposing thickness variation; i.e. the thickness-independent velocity image correctly represents the microstructural condition because the superimposing thickness variation has been eliminated in the image.

To determine the nature of the microstructural variation, another abrasive cut-off wheel showing a similar thickness-independent velocity was cross-sectioned and examined optically. Figure 7 shows optical micrographs at relatively high (center) and low (area surrounding center) velocity cross-sectional locations of the wheel. The creviced, very dark areas indicate pores. The low velocity section appears significantly more porous (less dense) than does the high velocity section. As stated in the introductory section, density variation is known to occur in grinding wheels, and velocity has been shown to correlate in a positive linear fashion with density for a given material (Roth, et al., 1991). Thus, the thickness-independent velocity image is mapping the density variation condition in the wheel and the central region of the wheel is indicated by the velocity image to contain a large area of high density as compared to surrounding regions. Since increasing thickness and increasing density are present in the center of the wheel and these effects are known to be complementary for radiography, the x-ray transmission density (Equation (6)) decrease in the wheel center shown in Figure 6c is ambiguous in its underlying nature. A detailed analysis of the radiographic results is required to determine whether thickness and/or density is the dominating effect. An example of how to complete such an analysis is shown in the Appendix and it requires that the exact composition of the material be known. As a consequence of the thickness-independent velocity imaging showing the true microstructural condition of the abrasive cut-off wheel, the industrial partner in this investigation is considering the use of the thickness-independent ultrasonic method as an industrial quality control tool. Ideally, the

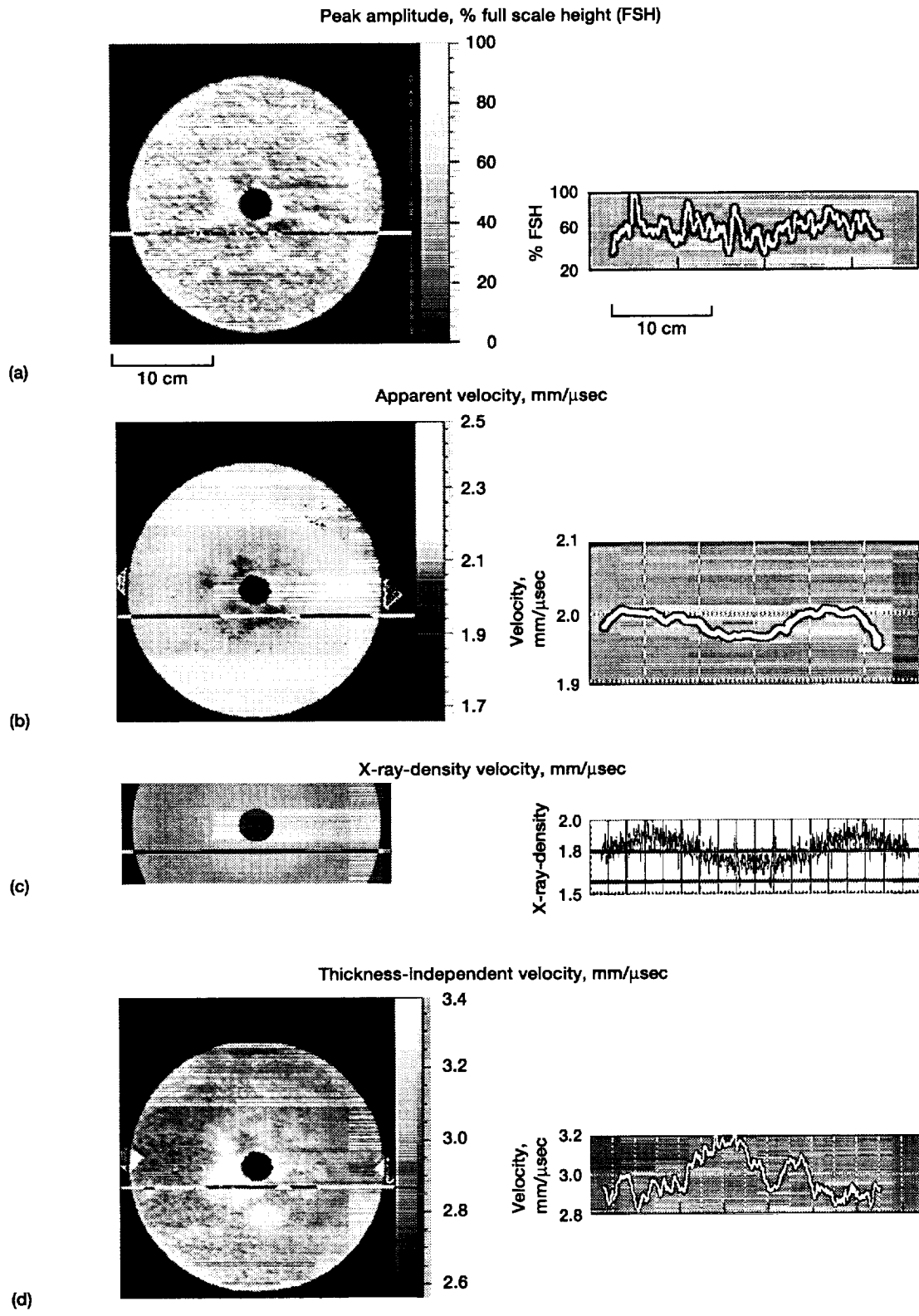


Figure 6.—NDE images and corresponding line profiles at horizontal position near the center of the abrasive cut-off wheel. (a) Conventional pulse-echo ultrasonic c-scan peak amplitude image (B1 gated) and peak amplitude line profile. (b) Apparent velocity image and velocity line profile. (c) Film radiograph of the left section and x-ray density line profile. (d) Thickness-independent ultrasonic velocity image and velocity line profile.

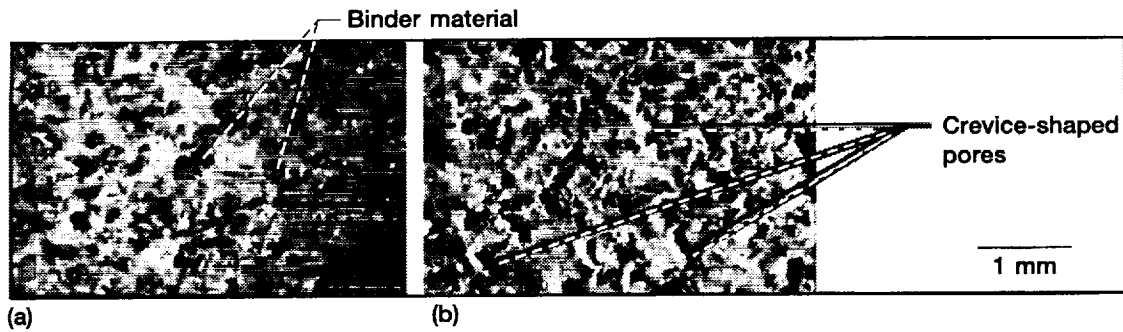


Figure 7.—High density/high velocity and low density/low velocity sections of wheel D10T4. (a) High density/high velocity section. (b) Low density/low velocity section.

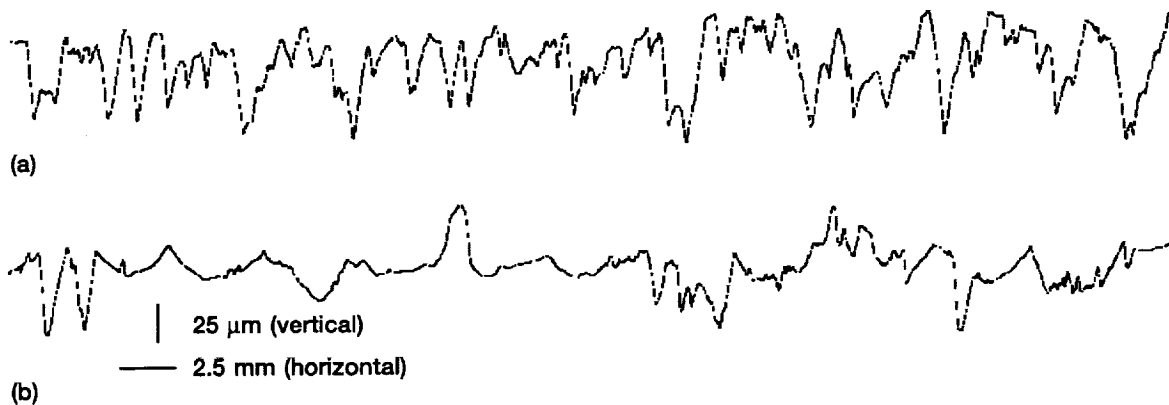


Figure 8.—Diamond-tip surface profiles at two areas of the abrasive cut-off wheel. (a) More finely spaced roughness. (b) More coarsely-spaced roughness.

use of this method or a variant of it for in-process control is desired to detect and fully characterize density variation within the wheel in the early stages of the wheel manufacturing process.

#### Further Discussion

For the low frequency (2.25 MHz broadband) examination of the cut-off wheel, peak amplitude response of the gated back surface echo B1 is likely dominated by density and surface roughness effects (although focused beams reduce the effect of surface roughness (Green and McIntire, 1991)) rather than thickness effects (Roth, 1997). Close examination of the peak amplitude and thickness-independent velocity images reveals some, though not easily observed, correlation between the two images; in some instances, areas of higher peak amplitude correlate with areas of higher velocity/higher density. This is consistent with prior investigations where increased ultrasonic transmission correlated with increased density (Roth, et al., 1995). Additionally, as mentioned in the Materials section, the abrasive cut-off wheel had noticeable surface roughness variations between portions of the central and surrounding regions. Examples of the different surface conditions for two areas of the wheel are shown in Figure 8. At many locations, the surface roughness variations appeared to correlate with density variation; a higher density/velocity region is located under a smoother surface portion. The dual effects complicate the analysis of the peak amplitude image. It is likely that the surface roughness variations present on both sides of the wheel caused ultrasonic scattering differences resulting in the amount of sound transmitted into the front surface and reflected from the back surface of the wheel to vary based on the surface condition. Generazio (1985), has shown that as the peak-to-valley surface roughness was increased from 0.1 to 1.5  $\mu\text{m}$  in a nickel 200 sample, and with an ultrasonic wavelength of  $\sim 30$  to  $70 \mu\text{m}$  impinging on the sample from the ultrasonic coupling medium, the reflection coefficient generally (but not in all cases) increased allowing less ultrasound to enter into the sample. This result is consistent with that for the cut-off wheel where as front surface roughness increased dramatically at locations in the region surrounding the central region, lower peak amplitude was observed in the peak amplitude image indicating less ultrasound likely

entering in these regions. Back surface roughness will also affect the peak amplitude of B1 (Green and McIntire, 1991). It is the experience of these authors that ultrasonic time-of-flight/velocity is not nearly as sensitive to surface roughness condition as is peak amplitude/attenuation in terms of percent change in value with change in surface condition.

## CONCLUSION

The single transducer thickness-independent ultrasonic imaging method was shown to precisely characterize the extent of the density variation in an abrasive cut-off wheel having a superimposing thickness variation. Conventional nondestructive evaluation methods are inaccurate in their attempts at characterizing the density variation because of the superimposing thickness variation. As a consequence of these results, the industrial partner in this investigation is considering the use of the thickness-independent ultrasonic method as an industrial quality control tool. Ideally, the use of this method or a variant of it for in-process control is desired to detect and fully characterize density variation within the wheel in the early stages of the wheel manufacturing process. This article has demonstrated a technology transfer of an advanced aerospace nondestructive evaluation method from NASA Lewis Research Center to the abrasives industry.

## REFERENCES

- Dayal, V.: An Automated Simultaneous Measurement of Thickness and Wave Velocity by Ultrasound, **Experimental Mechanics**, September, 1992, Vol. 32 No. 2, pp. 197–202.
- Generazio, E.R., The Role of the Reflection Coefficient in Precision Measurement of Ultrasonic Attenuation, **Materials Evaluation**, Vol. 43, No. 8, pp. 995–1004, 1985.
- Halmshaw, R, Industrial Radiology, Theory and Practice, Applied Science Publishers, p. 31, 1982.
- Hsu, D.K. and Hughes, M.S.: Simultaneous ultrasonic velocity and sample thickness measurement and application in composites. **J. Acoust. Soc. Am.** Vol. 92, No. 2, Pt. 1, Aug. 1992, pp. 669–675.
- Hubbell, J.H., Photon Cross Sections, Attenuation Coefficients, and Energy Absorption Coefficients From 10 keV to 100 GeV, NSRDS-NBS 29, Center for Radiation Research, National Bureau of Standards, August, 1969.
- Hubbell, J.H., Photon Mass Attenuation and Energy-Absorbing Coefficients from 1 keV to 20 MeV, **Int. J. Appl. Radiat. Isot.**, Vol. 33, pp. 1269–1290, 1982.
- Hughes, M.S. and Hsu, D.K.: An automated algorithm for simultaneously producing velocity and thickness images, **Ultrasonics**, 1994 Vol. 32 No. 1, pp. 31–37.
- Kuo, I.Y., Hete, B. and Shung, K.K.: A novel method for the measurement of acoustic speed. **J. Acoust. Soc. Am.** Vol. 88, No. 4, Oct. 1992, pp. 1679–1682.
- Macovski, A., **Medical Imaging Systems**, Prentice-Hall, Inc., 1983, pp. 23–35, 106–144.
- NASA Strategic Plan, TM–110592, 1995.
- NASA Tech Briefs, April 1997, pp. 30–32.
- Nondestructive Testing Handbook, second edition, Volume 7 Ultrasonic Testing, eds. Birks, A.S., Green, R.E., and McIntire, P. American Society For Nondestructive Testing, 1991, pp. 405, 225, 229–230, 254, 258.
- Pichè, L.: Ultrasonic velocity measurement for the determination of density in polyethylene. **Polymer Engineering and Science**, Vol. 24, No. 17, Mid-December 1984, pp. 1354–1358.
- Roth, D.J., et. al.: Scaling up the Single Transducer Thickness-Independent Ultrasonic Imaging Method for Accurate Characterization of Microstructural Gradients in Monolithic and Composite Tubular Structures. NASA TM–1998-206625, 1998.
- Roth, D.J.: Using a Single Transducer Ultrasonic Imaging Method to Eliminate the Effect of Thickness Variation in the Images of Ceramic and Composite Plates, **J. Nondest. Eval.**, Vol. 16, No. 2, June 1997.
- Roth, D.J., et. al.: Commercial Implementation of Ultrasonic Velocity Imaging Methods via Cooperative Agreement Between NASA Lewis Research Center and Sonix, Inc. NASA TM–107138, 1996.
- Roth, D.J., et. Al., An NDE Approach for Characterizing Quality Problems in Polymer Matrix Composites, Proceedings of the 40<sup>th</sup> International SAMPE Symposium, May 8–11, 1995 and NASA TM–106807.
- Roth, D.J., Stang, D.B., Swickard, S.M., DeGuire, M.R., and Dolhert, L.E.: “Review, Modeling and Statistical Analysis of Ultrasonic Velocity-Pore Fraction Relations in Polycrystalline Materials,” **Mater. Eval.**, Vol. 49, No. 7, July 1991, pp. 883–888.
- Sollish, B.D.: Ultrasonic Velocity and thickness gage, United States Patent No. 4,056,970, Nov. 8, 1977.

## APPENDIX

To determine if a portion of the x-ray density variation might be due to microstructural variation in addition to the thickness variation, the following analysis needs to be performed which is good to a first approximation. The following will show a sample analysis for a silicon nitride ceramic material ~0.7 cm thick with a 10% thickness variation. Equation (1) in the body of the text can be expressed in terms of X-ray intensity transmission (I) and x-ray linear attenuation coefficient ( $\mu$ ) according to (Macovski, 1983):

$$I = I_0 \exp(-\mu d) \quad (\text{A1})$$

where  $I_0$  is the incident x-ray beam intensity and  $d$  is thickness. Setting up a ratio of transmission intensities for thickness difference is required while assuming a uniform linear attenuation ( $\mu$ ) coefficient:

$$\frac{I_2}{I_1} = \frac{\exp(-\mu[d - 0.1d])}{\exp(-\mu d)} = \exp(0.1\mu) = \exp([0.1][0.9735][0.7\text{cm}]) = 1.071 \quad (\text{A2})$$

where 0.9735 is the effective x-ray linear attenuation coefficient ( $\mu$ ) in silicon nitride for 45 kV tube voltage (30 kV effective voltage) and 0.7 cm is the ~thickness of silicon nitride the x-ray beam traveled through. (Obtaining linear attenuation coefficient for a material requires exact composition and is calculated from a rule of mixtures approach with the first step calculating the mass attenuation coefficient ( $\mu/\rho$ ) for the compound from (Hubbell, 1969):

$$\mu = \left( \sum w_i \frac{\mu_i}{\rho_i} \right) \left( \sum w_i \rho_i \right) \quad (\text{A3})$$

where  $w_i$ ,  $\mu_i/\rho_i$  and  $\rho_i$  are the proportion by weight, mass attenuation coefficient, and density, respectively, of the  $i$ th element.  $\mu/\rho$  and  $\rho$  for the elements have been tabulated in various references (Hubbell, 1969; 1982). The *expected* x-ray transmission density difference ( $\Delta XD$ ) (see Equation (6) in the body of the text) between the thinner and thicker material sections based on the results of Equation (A2) can be computed from:

$$\Delta XD = G_D \log_{10} \frac{I_2}{I_1} = 3 \log_{10}(1.071) = 0.089 \quad (\text{A4})$$

where  $G_D = 3$  is the type M film gradient. The *observed* ( $\Delta XD$ ) for the silicon nitride material was  $XD_1 - XD_2 = 2.9 - 2.7 = 0.2$  where  $XD_1$  and  $XD_2$  were the x-ray transmission densities for the thinner and thicker sections of material, respectively. The observed value for x-ray transmission density difference of 0.2 is ~ twice the expected value of 0.089 computed using Equation (A4). This indicates that microstructural variation such as physical density/ pore fraction variation in addition to thickness variation was responsible for the x-ray density variation in the silicon nitride. Specifically, the observed x-ray density results indicate that the thinner section most likely had lower physical density than did the thicker section because the thinner section showed higher x-ray density.



**REPORT DOCUMENTATION PAGE**Form Approved  
OMB No. 0704-0188

Public reporting burden for this collection of information is estimated to average 1 hour per response, including the time for reviewing instructions, searching existing data sources, gathering and maintaining the data needed, and completing and reviewing the collection of information. Send comments regarding this burden estimate or any other aspect of this collection of information, including suggestions for reducing this burden, to Washington Headquarters Services, Directorate for Information Operations and Reports, 1215 Jefferson Davis Highway, Suite 1204, Arlington, VA 22202-4302, and to the Office of Management and Budget, Paperwork Reduction Project (0704-0188), Washington, DC 20503.

1. AGENCY USE ONLY (Leave blank)		2. REPORT DATE August 1998	3. REPORT TYPE AND DATES COVERED Technical Memorandum	
4. TITLE AND SUBTITLE Thickness-Independent Ultrasonic Imaging Applied to Abrasive Cut-Off Wheels: An Advanced Aerospace Materials Characterization Method for the Abrasives Industry: A NASA Lewis Research Center Technology Transfer Case History			5. FUNDING NUMBERS  WU-523-21-13-00	
6. AUTHOR(S)  Don J. Roth and Donald A. Farmer				
7. PERFORMING ORGANIZATION NAME(S) AND ADDRESS(ES)  National Aeronautics and Space Administration Lewis Research Center Cleveland, Ohio 44135-3191			8. PERFORMING ORGANIZATION REPORT NUMBER  E-11210	
9. SPONSORING/MONITORING AGENCY NAME(S) AND ADDRESS(ES)  National Aeronautics and Space Administration Washington, DC 20546-0001			10. SPONSORING/MONITORING AGENCY REPORT NUMBER  NASA TM-1998-207924	
11. SUPPLEMENTARY NOTES  Don J. Roth, NASA Lewis Research Center, and Donald A. Farmer, Allison Abrasives, Inc., 163 Industry Rd., Lancaster, Kentucky 40444. Responsible person, Don J. Roth, organization code 5920, (216) 433-6017.				
12a. DISTRIBUTION/AVAILABILITY STATEMENT  Unclassified - Unlimited Subject Category: 38  This publication is available from the NASA Center for AeroSpace Information, (301) 621-0390.			12b. DISTRIBUTION CODE  Distribution: Nonstandard	
13. ABSTRACT (Maximum 200 words)  Abrasive cut-off wheels are at times unintentionally manufactured with nonuniformity that is difficult to identify and sufficiently characterize without time-consuming, destructive examination. One particular nonuniformity is a density variation condition occurring around the wheel circumference or along the radius, or both. This density variation, depending on its severity, can cause wheel warpage and wheel vibration resulting in unacceptable performance and perhaps premature failure of the wheel. Conventional nondestructive evaluation methods such as ultrasonic c-scan imaging and film radiography are inaccurate in their attempts at characterizing the density variation because a superimposing thickness variation exists as well in the wheel. In this article, the single transducer thickness-independent ultrasonic imaging method, developed specifically to allow more accurate characterization of aerospace components, is shown to precisely characterize the extent of the density variation in a cut-off wheel having a superimposing thickness variation. The method thereby has potential as an effective quality control tool in the abrasives industry for the wheel manufacturer.				
14. SUBJECT TERMS  NDE; Nondestructive evaluation; Ultrasonics; Ultrasonic velocity; Thickness			15. NUMBER OF PAGES 16	
			16. PRICE CODE A03	
17. SECURITY CLASSIFICATION OF REPORT Unclassified	18. SECURITY CLASSIFICATION OF THIS PAGE Unclassified	19. SECURITY CLASSIFICATION OF ABSTRACT Unclassified	20. LIMITATION OF ABSTRACT	